euspen's 22nd International Conference & Exhibition, Geneva, CH, May/June 2022
www.euspen.eu

Minimization of kinematic complexity while diamond machining of curved diffraction gratings

M. Jagodzinski[1], S. Kühne[1], D. Rolon[1], M. Malcher[1], D. Oberschmidt[1]

[1] *Technische Universität Berlin, Department Micro and Precision Devices MFG, Germany*

jagodzinski@mfg.tu-berlin.de

Abstract

The rising demand for compact, cost-effective optical measurement devices like dispersion spectrometers poses a driving force for the availability of diffractive optical elements with high efficiency. The diffractive elements used are typically blazed gratings, which, in order to enable high resolution and imaging quality, need to be manufactured on curved samples. The lithographic or holographic methods often used are state of the art technologies that turns the production of high-efficient, aberration correcting gratings feasible. Nevertheless, the high demands concerning setup time and restrictions of manufacturable grating microgeometries limit the production of certain grating geometries.

An alternative approach for complex grating manufacture is multi-axis ultra-precision diamond machining in which the curved grooves are cut sequentially. However, the inclusion of multiple rotary axes comes at the cost of increasing geometrical inaccuracies as the axis imperfections accumulate into random errors of groove positions which cause an increase in straylight and related SNR. Thus, the minimization of machine tool axes is a viable approach for complex optics manufacture but comes at the expense of geometrical deviations and related optical performance. Hence, the machine tool kinematics have to be selected or configured with regard to the resulting and demanded optical performance.

The presented work encompasses aspects of a complexity-reduced manufacture without rotary axis of curved blazed diffraction gratings and the resulting optical performance. A LT-Ultra MMC1100 machine tool was used for the evaluation of imperfections of the machine axes and resulting geometries. The investigated diffractive elements are blazed diffraction gratings with a groove period of b = 3 µm, radius of curvature R = 75 mm, diameter d = 12.5 mm and various degrees of freedom. The experimental results show low deviations compared to numeric and analytical models. The optical parameters determined by laser-scatterometry show resulting diffraction efficiencies of η ~ 60 % and SNR < 1E-3.

Diffractive optics, Ultra-precision, Microstructure, machine-tool kinematics

1. Introduction

Optical spectrometers perceive a trend towards minimization and/or miniaturization. Although MEMS-devices and Fourier transform spectroscopes enable the production of small, cost-effective systems, diffraction grating spectroscopes are still in use. Especially if high spectral or imaging resolution is demanded, imaging diffractive optical elements (iDOE) are used which comprise imaging as well as diffractive properties. This enables the reduction of necessary optical components and related system complexity. By the use of concave diffraction gratings only one single optical component might be integrated into the optical mount [1]. Compared to other, more complex optical mounts reflection losses as well as instrument straylight are reduced but optical aberrations like astigmatism and image curvature are less compensated. An aberration correction can be, at least partially, compensated by non-linear trajectory of the grooves of the concave grating so that those are not equidistant aligned but curved orthogonal to the optical axis of the element, as depicted in Figure 01. This kind of complex geometry can be produced by advanced techniques of interference lithography (IFL) [2] and, to some degree, by classical ruling machines. Yet, IFL is a very time-consuming, exhaustive process and classical ruling machines are limited in the variety of achievable tool paths. As an alternative to classic ruling machines, multi-axis ultra-precision machine tools offer positioning accuracies that increasingly meet requirements in the nanometer range. Due to NC-Machine axis control almost arbitrary tool paths [3, 4] are possible. As no optical IFL-setup needs to be built and designed, production times can be reduced to few hours or days. However, as complex, rotational kinematics are associated with increased process and product disturbances, which lead to elevated straylight and lower signal-to-noise-ratio, the manufacturing kinematic should be reduced to a minimum of needed machine axes.

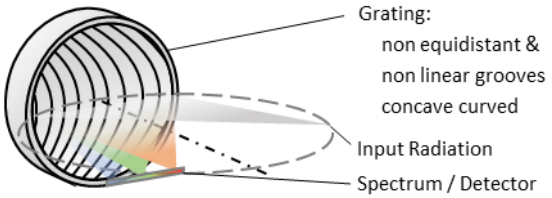

Figure 01. Concave grating mount

The minimum possible kinematic for manufacture of curved diffraction gratings with non-equidistant and axial curved grooves is a 3-axis translational kinematic. Minimizing the kinematic by eliminating the rotational degrees of freedom is associated with geometrical deviations of the nominal geometry and related losses of optical performance. Therefore, the manufacture of complex curved diffraction gratings is a compromise between geometric complexity and minimization of process disturbances which has to be met by the requirements of the particular diffraction grating. This paper aims at investigating the optical gains and losses of a minimized machine kinematic for the machining of concave gratings with complex groove geometry for aberration correction.

2. Scenario and Experimental setup

2.1. Optical concave grating mount

For the investigation of the kinematic influences on the grating properties a concave grating mount has been chosen, depicted in Figure 02. The design and optimization are done by ray tracing in ZEMAX OPTIC STUDIO. The triangular, blazed groove geometry parameters are selected for the use in VIS and offer machinability via shaping with rectangular diamond tools. The radius of the grating corresponds to the lower end of the radii of commercially available IFL produced diffraction gratings. The element comprises a non-linear phase function which enables the correction of astigmatism for the central wavelength and results in slightly curved, non-equidistant grooves.

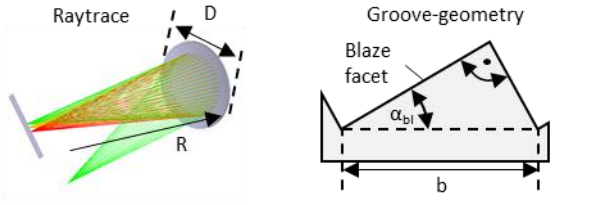

Mount:	Rowland	Criteria	
Radius R:	75 mm	Wavelength λ:	632.8 nm
Diameter D:	12.5 mm	Signal-to-Noise-Ratio SNR:	< 1E-4
Groove width b:	3 µm	F-number k:	< 6.22
Blaze-angle α_{bl}:	6 °	Diffraction efficiency η_m:	> 50 %

Figure 02. Design and parameters for the investigated grating type

2.2. Experimental setup

The manufacture of the experimental diffraction gratings was conducted on a MMC1100 ultraprecision machining center from LT ULTRA-PRECISION TECHNOLOGY GMBH, Herdwangen-Schönach, Germany (see Figure 03). The 3-axis machine kinematics is extended with a tilt/turn module with two serial rotary axes. As each groove is cut sequentially, the tool geometry must match the groove geometry and quality [3], so that rectangular shaped, monocrystalline diamond tools were used.

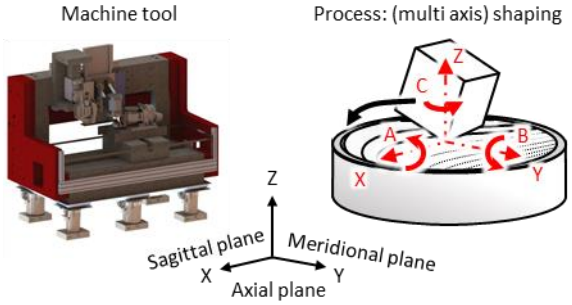

Axes	X,Y,Z, A,C
Base, bearings	Granite, hydrostatic bearing
Measurement system	Glas scales
Positional resolution	X, Z: 25 nm | Y: 1 nm | A: 5" | C: 3"
Material	RSA-501

Figure 03. Machine tool and degrees of freedom

For the acquisition of the optical properties of the experimental gratings, in particular stray light behaviour as well as diffraction efficiency, a custom-built laser scatterometer, depicted in Figure 04, was designed and realized. The beam source of the instrument is a polarized helium-neon laser with 5 mW continuous wave power with adaptable polarization orientation via a λ½ plate. The illumination intensity is adjusted by means of neutral density filters, which enable spatially correlated intensity measurements with an avalanche-photodiode over up to 6 orders of magnitude. The use of a beam splitter plate results in an autocollimation measurement of reflected (scattered) radiation which closely resembles the optical alignment of concave grating mounts, in which a diffraction order with low diffraction angle is used. The sample is mounted on a goniometer unit and is adjustable in 5 degrees of freedom by means of a manual translation-rotation stage.

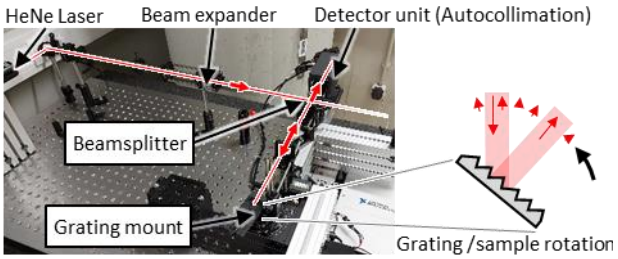

Figure 03. Custom built Scatterometer setup

2.3. Kinematics considerations

The optical functionality and performance of diffraction gratings is closely related to the positional accuracy of the trajectories as well as the profile of the grooves. In particular, the blaze angle determines the diffraction efficiency, whereas the groove positional accuracy relates to the stray-light-level. Therefore, in order to achieve a minimal deviation of nominal and machined geometry, diamond machining requires an adequate guidance of the diamond tools with sharp rectangular cutting edge. A curvature of groove trajectories in the axial plane as well as surface curvature in the sagittal plane might require additional rotational axes in order to prevent damage to the workpiece by the side clearance faces of the diamond tool. A cartesian scheme of this is shown in Figure 03, in which the machining kinematics contains three translational (X, Y, Z) and 3 orthogonal, rotational degrees of freedom (A, B, C). The blaze angle of the grooves determines the diffraction efficiency η_m which is the ratio of incident and diffracted radiation. As the blaze angle is defined in relation to the local slope of the grating surface, at least one rotational machine axis is required for rotational alignment of the diamond tool which is demonstrated in [3] and depicted in Figure 05-A.

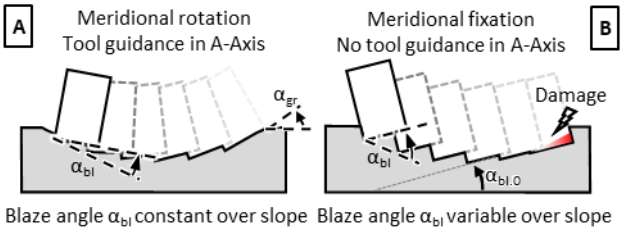

Figure 05. Meridional rotation(A) and fixation (B) of the diamond tool

However, this still is related to a finite amount of machining precision, as finite axis stiffness and tool alignment precision cause random as well as non-corrected systematic errors in the grating grooves. Therefore, enhanced straylight and wavefront deviations are expected with this kind of tool guidance. By meridional fixation of the tool, as shown in Figure 5-B, much less tool positioning disturbances are expected, as the tool is typically mounted on a stiff fixure and no rotational axis is implemented in this spatial plane. However, if the local surface slope exceeds the mean blaze angle $\alpha_{bl.0}$ contour damage of adjacent grooves occurs, depicted in Figure 5-B. Therefore, the mean blaze angle must exceed the maximum surface tangential angle α_{gr}. The surface slope needs to be considered in the sagittal plane as well. If the clearance angle of the cutting tool does not suffice the maximum surface tangential angle, a rotational B-Axis must be implemented. As the curvature at the edge of the grating surface $\alpha_{gr} \leq 4.5°$ is lower than the blaze angle $\alpha_{bl} = 6°$ as well as the clearance angle $\alpha_f = 5°$ of the used

diamond tools, rotations within the axial and sagittal plane are not necessary for the designed grating. In addition, the curvature of the grooves in the axial plane for aberration reduction has been found to be $\gamma_{traj} < 5°$ which can be manufactured with a side clearance angle $\alpha_p \geq 5°$ without any need for axial rotation. Therefore only the meridional rotation of the tool poses a potentially necessary degree of freedom, so that the corresponding influence on the resulting diffraction efficiency of the grating needs to be examined.

3. Theoretical approach

3.1. Diffraction efficiency

Minimized machining relates to a change of the blaze angle and related diffraction efficiency over the grating surface. In order to determine the influence of the blaze angle on the diffraction efficiency numerical calculations by Fourier-modal-method with the diffraction-grating toolbox of the optics design Software VIRTUALLABS FUSION were conducted. The influence of the blaze angle on the calculated diffraction efficiency is depicted in Figure 06. The diffraction efficiency amounts a maximum value of $\eta_{max} \approx 0.85$ at a blaze-angle $\alpha_p \approx 6°$ and is nearly independent of the polarization. However, the already slight deviations of few degrees of the optimal blaze angle cause significant losses of the diffraction efficiency.

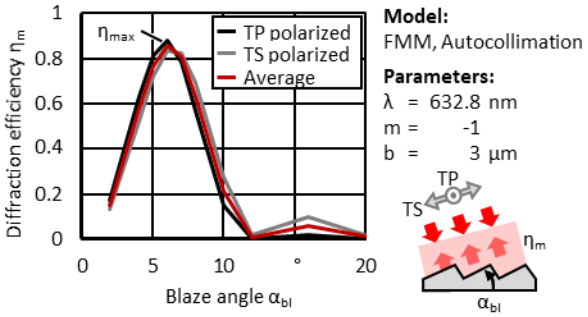

Figure 06. Calculated diffraction efficiency

Regarding curved gratings with meridional fixation, changes of the blaze angle cause local variations of the diffraction efficiency so that the total amount of diffracted intensity differs from that of a grating with meridional tool rotation. The resulting diffraction efficiency η_{res} of a mounted grating is to be determined by integration of the local diffraction efficiency η_m over the grating surface. Therefore a mean blaze angle has to be selected which enables a maximum level of resulting diffraction efficiency, depicted in Figure 07. As the minimum manufacturable mean blaze angle increases for lower f-numbers, optimum blaze angles might not be manufacturable, so that the resulting diffraction efficiency is reduced for those optics. This means that a diffraction efficiency of $\eta_{res} \geq 0.5$ is only achievable for higher f-numbers. As the optical mount contains a f-number k = 6.22, a resulting diffraction efficiency of $\eta_{res} = 0.61$ is theoretically achievable by meridional fixation.

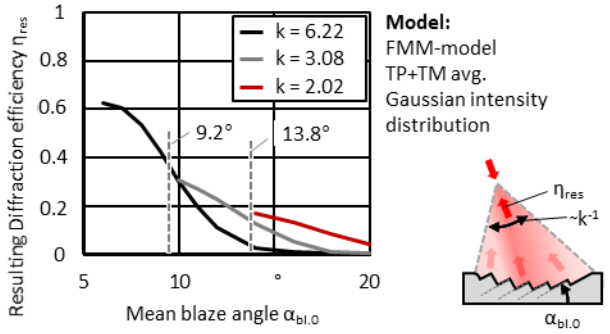

Figure 07. Calculated resulting diffraction efficiencies for curved reflective gratings

3.2. Stray light modeling

The level of straylight between the diffraction orders is a relevant quantity of grating spectrometers as this influences the achievable signal-to-noise-ratio (SNR). According to a straylight theory formalized SHARPE and IRISH [5] the intensity distribution between the diffraction orders can be attributed to four individual components. Those straylight components are determined by the illumination conditions (η_{il}), variations of the groove width (η_{br}) and the groove depth (η_{de}), as well as the roughness Rq of the blaze facets (η_{ro}). According to [5], the scattered light components form the relative stray light portion η_{str} of the corresponding diffraction order (m = 1):

$$\eta_{str} = \eta_{il} + \eta_{br} + \eta_{de} + \eta_{ro} \qquad (1)$$

The straylight components are depicted in Figure 08. The geometrical parameters are determined from AFM-Metrology of experimental gratings. The variation of the groove width is of least importance, since the illumination- and roughness-related straylight components η_{il}, η_{ro} have a larger influence. Nevertheless, both straylight components are still an order of magnitude below the straylight component of variations in groove depth η_{de}, so η_{il} and η_{ro} these are also considered negligible in the given parameter range. The dominating straylight component is η_{de}, is related to the standard deviation of the groove depths σ_{de}. For the depicted values σ_{de} = 3 nm was assumed, as this can be expected as translational positioning accuracy of state of the art ultraprecision machines, which is in good accordance to measured values of experimentally cut gratings with three translational axes.

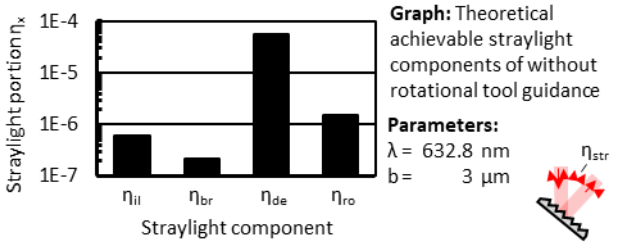

Figure 08. Calculated portions of the straylight components

However, an increased standard deviation of the groove depth is found when the A-axis of the experimental machine is involved in the cutting process. By regression of a step sequence on AFM measurements of planar gratings, exemplarily shown in Figure 09, the height of the groove facets h_{fl} was determined. The corresponding standard deviation of the distance of the blaze facets is $\sigma_{fl} > 5.2$ nm. For near-normal incident angles and small diffraction angles it can be assumed to be nearly identical to the standard deviation $\sigma_{fl} = \sigma_{de} > 5.2$ nm of the groove depths [5]. Therefore, a higher straylight level is to be expected for gratings cut with this axis, especially, as the straylight component is proportional to the square of the standard deviation of the groove depth $\eta_{de} \sim \sigma_{de}^2$.

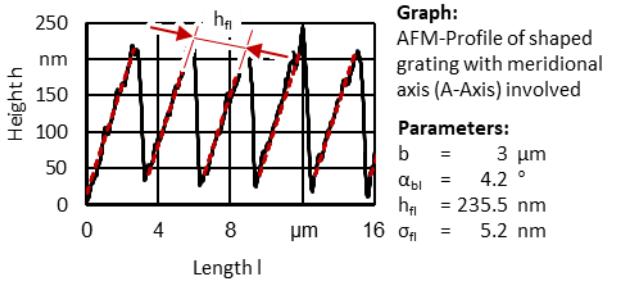

Figure 09. Exemplary AFM-Profile

3.3. Assessment of kinematic configuration

As the SNR is an important value for spectroscopic systems, optimal optical properties of the diffraction gratings are achieved by machine kinematics that contain the lowest possible number of rotational axes while ensuring the best possible fulfilment of the requirements of the optical specifications. As the maximum achievable diffraction efficiency η_{max} poses the achievable limit, the normalized diffraction efficiency $\eta_{res.norm}$ is introduced:

$$\eta_{res.norm} = \frac{\eta_{res}}{\eta_{max}} \qquad (2)$$

In Figure 10 a comparison of achievable levels of diffraction efficiency and straylight is depicted. Gratings with $k > 6.22$ enable a normalized resulting diffraction efficiency of $\eta_{res.norm} > 0.72$. Lower f-numbers lead to higher variations of the blaze angle over the surface, resulting in significantly lower resulting diffraction efficiencies. Already for a f-number of $k = 3.125$, the resulting diffraction efficiency of the grating is halved to $\eta_{res.norm} = 0.36$. Therefore, gratings with f-numbers $k \lessapprox 5$ are considered to require the integration of a rotational A-axis, since the blaze angle can be kept constant over the surface by rotational guidance of the tool. However, although this maximizes the resulting diffraction efficiency, an increase of the straylight η_{str} by at least factor 2.9 (almost half an order of magnitude) is to be expected. Therefore, in order to match the requirements, a minimal kinematic with three translational axes is to be selected for the production of a concave grating with minimal stray light.

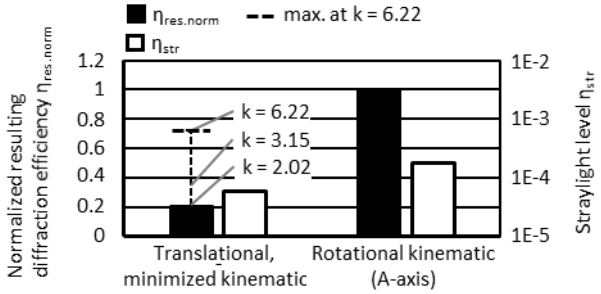

Figure 10. Comparison of minimal kinematic with rotational kinematic

4. Optical measurement results

A concave grating with complex groove geometries was fabricated without meridional tool rotation. The diffraction efficiency measured locally across the meridional plane is shown in Figure 11-A. It can be seen that there is a variation in diffraction efficiency across the grating surface. The graphs from FMM model and experimentally determined measured values are sufficiently matching around the central region of the grating. The maximum measured dispersed intensity is found at $\alpha_{bl} \approx 6°$, which is predicted by the FMM model. Deviations of the trajectories are observed at blaze angles $\alpha_{bl} \gtrapprox 7°$ which can be explained by finite adjustment accuracy and artefacts of the measurement setup. Furthermore, a finite measurement spot size with diameter $d_{spot} = 2$ mm was used for the measurement. In the edge region of the grating surface, part of the laser radiation thus is not incident on the grating surface, so that measurement artefacts are to be expected there. The element demonstrates the loss of dispersed power when the rotational degree of freedom is fixed. The dispersed intensity of the element is more than half (58%) of what would be achievable with rotational guidance. The measured and calculated curves of the straylight of the experimental grating are depicted in Figure 11-B. The deviations of measured and calculated values are below one order of magnitude. The measured stray light reaches a minimum of ca. 1.3 E-4 of the intensity of the diffraction order, which corresponds to a groove depth variation of ~ 6 nm for this particular grating. Although this measured value is slightly above the desired specification, it is still considered as the optimal optical performance, as for additional axes an even higher stray light level would occur.

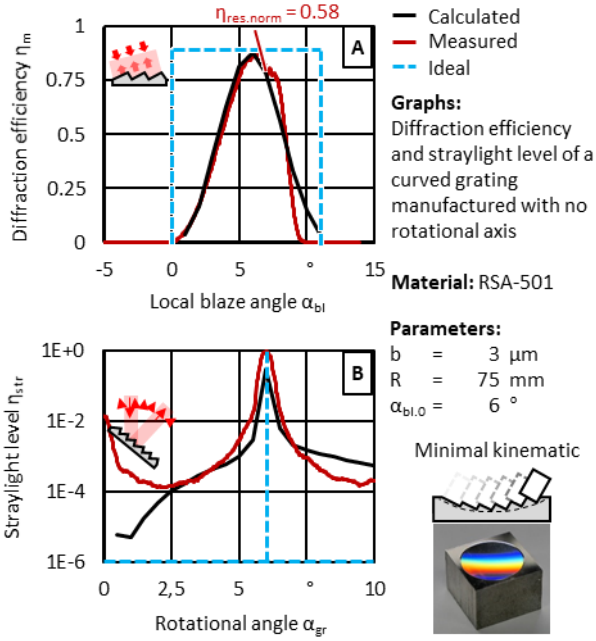

Figure 11. Comparison of measured and calculated optical performance of a concave diffraction grating

5. Conclusions

On the basis of an exemplary ultra-precision machine, the optical parameters and performance values were determined and correlated to the manufacturing kinematics. The experimental results sufficiently comply to theoretical values with a diffraction efficiency of $\eta_{res} = 58\%$ and a straylight level below three orders of magnitude. The connection between optical properties and manufacturing strategy allows an assessment of feasibility and expectable performance of imaging diffractive gratings with minimal complexity of the kinematics. The results also serve as a guidance for the manufacturer to select and potentially optimize the kinematics and machine tool. Thus, an approach towards production of curved diffraction gratings with a property profile tailored to the target application is provided.

Acknowledgement

We thank our colleagues at the Department of Optics and Atomic Physics of the Berlin Institute of Technology, in particular Karsten Pufahl, for support with the simulations with Zemax Optic Studio

References

[1] Rowland, H. A.: On concave gratings for optical purposes. American Journal of Science 152/s3-26, S. 87–98, 1883.

[2] Glaser, T.: High-end spectroscopic diffraction gratings. Design and manufacturing. *Advanced Optical Technologies* **4** (2015) (1), p.25-46

[3] Kühne, S.: Ultrapräzisionsverfahren zur Erhöhung der Güte abbildender Beugungsgitter, Fraunhofer Verlag 2018

[4] Clercq, C. de et al.: ELOIS: an innovative spectrometer design using a free-form grating., Optical Systems Design 2015: Optical Design and Engineering VI., SPIE, 96261O, 2015.

[5] Sharpe, M.R., Irish, D: Stray Light in Diffraction Grating Monochromators. Optica Acta: International Journal of Optics 9/25, S. 861–893, 1978.